Recently, the metal/glass fibre, in which a large D-shaped hole is introduced in the cladding, has been proposed, and in a short period of time it has found many interesting applications in fibre devices, such as fibre polarisers and fibre lasers.[3] However, until now the modal birefringence of this fibre, in which no metal is inserted, has not been investigated. The purpose of this letter is to clarify its geometrical birefringence in detail.

Analysis: This fibre comprises three regions: core, cladding and D-shaped hole. The parameters R_0, a and r_1 are the radius of the cladding, core and D-shaped hole, respectively, and d is the core/flat distance. Using the improved H-field FEM[4] in which the condition $\nabla \times \boldsymbol{H} = 0$ is satisfied in the least-squares sense, the spurious solutions, which appear in the case of the E_z–H_z FEM, do not occur in the guided mode region, and thus the propagation constants of the guided mode can be calculated.

In the improved H-field FEM, only half of the cross-section is divided into a number of second-order triangular elements because of symmetry. Double precision has been adopted in all computations to avoid roundoff error. Figs. 1, 2 and 3

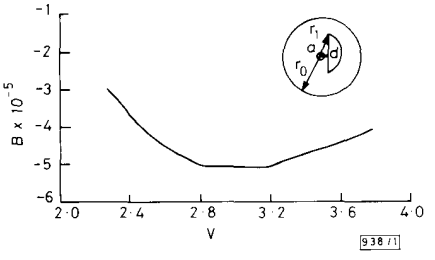

Fig. 1 *Dependence of geometrical birefringence on normalised frequency V*

$r_0/a = 20{\cdot}833$, $r_1/a = 8{\cdot}667$, $d/a = 2{\cdot}333$, $n_1 \simeq 1{\cdot}458$, delta = 0·008; $B = (\beta_x - \beta_y)/k$

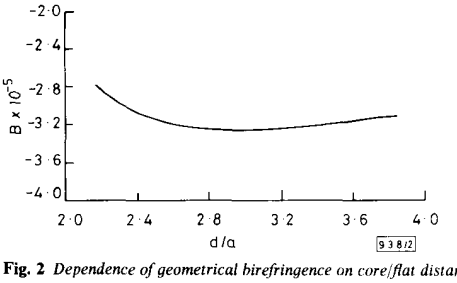

Fig. 2 *Dependence of geometrical birefringence on core/flat distance d*

$r_0/a = 20{\cdot}833$, $r_1/a = 8{\cdot}667$, $n_1 = 1{\cdot}458$, delta = 0·008, $\beta = 6{\cdot}000$

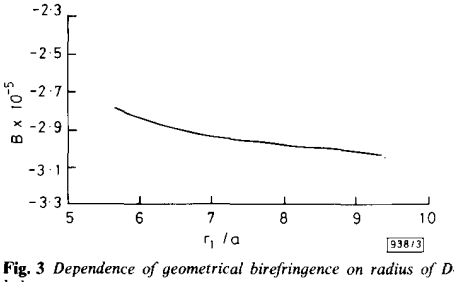

Fig. 3 *Dependence of geometrical birefringence on radius of D-shaped hole r_1*

$r_0/a = 20.833$, $d/a = 2{\cdot}333$, $n_1 = 1{\cdot}458$, delta = 0·008, $\beta = 6{\cdot}000$

show the dependence of geometrical birefringence on normalised frequency V, core/flat distance d and radius of the D-shaped hole, respectively. The following points are concluded from these results:

(1) The dependence of B_g on normalised frequency V is remarkable, especially in the single-mode region.

(2) B_g varies slightly with the geometrical parameters of the D-shaped hole. The larger the hole, the higher the birefringence. However, the modal birefringence reaches its highest value when the ratio of the core/flat distance to core radius is about 3.

(3) B_g is of the order of $4{\cdot}5 \times 10^{-5}$, and the corresponding beat length is approximately 1·4 cm at a wavelength of 633 nm.

In fact, the field of mode $E_{\|}^{y}$ is parallel to the flat boundary of the D-hole, and can hardly extend into the hole region. The field of $E_{\|}^{x}$ is perpendicular to the flat boundary, and therefore tends to go out into the hole region. Thus the influence of the flat boundary on the effective index is more remarkable for the mode $E_{\|}^{x}$ than for the mode $E_{\|}^{y}$. At a fairly high normalised frequency V, the fields are confined to the core region and the influence of the D-hole on B_g is negligible. However, when V is not very high ($V = 3 \sim 4$, for example), the fields will extend to the cladding region. Thus the birefringence will become large because of the different influence of the D-hole on the two orthogonal modes. If the frequency V becomes lower, the field will extend further into the cladding and the outer boundary of the D-hole will have its influence on the modes. However, the difference of influence on the two modes becomes small. Therefore the birefringence will be reduced in part again, and so the results given can be realised from these discussions.

In general, D-shaped hole fibres can be used not only as a special fibre for the making of many fibre devices, but can also maintain the linear polarisation state of the light.

Conclusions: The birefringence of D-shaped hole fibres is evaluated using the improved H-field FEM analysis. It is found that the magnitude of the geometrical birefringence is about $4{\cdot}5 \times 10^{-5}$, and that the linear polarisation state of the light can generally be maintained to some degree.

HONG JIN
QIAN JINGREN

University of Science & Technology of China
Hefei, Anhui 230026, People's Republic of China

20th September 1989

References

1 OKISHI, T.: 'Single-polarization single-mode optical fibers', *IEEE J. Quantum Electron.*, 1981, **QE-17**, pp. 879–884
2 NODA, J., OKOMOTO, K., and SASAKI, Y.: 'Polarization-maintaining fibers and their applications', *J. Lightwave Technol.*, 1986, **LT-4**, pp. 1071–1089
3 LI, L., WYLANGOWSKI, G., PAYNE, D. N., and BIRCH, R. D.: 'Broadband metal/glass single-mode fibre polarisers', *Electron. Lett.*, 1986, **22**, pp. 1020–1022
4 KOSHIBA, M.: 'Improved finite element formulation in terms of the magnetic field vector for dielectric waveguides', *IEEE. Trans.*, 1985, **MTT-33**, pp. 227–233

OPTICALLY CONTROLLED PHASE SHIFT OF SCHOTTKY COPLANAR LINES

Indexing terms: Microwave devices and components, Transmission lines, Phase-shifters, Optoelectronics

We present experimental results on the optically controlled properties of a coplanar Schottky-contact transmission line. It is shown that a phase shift of the order of 90 to 180°/cm is achieved by optically varying the width of the depletion layer, the device acting as a distributed Schottky photodiode.

Introduction: Many exciting developments have been seen in the last decade in the application of optical technology to microwave devices, circuits and systems. The optical generation and detection of ultrashort electrical pulses with frequency spectra extending from DC to THz has stimulated a

large number of applications in microwave measurement techniques.[1] At the same time, a large amount of effort has been devoted to the optical control of semiconductor devices.[2,3] Here the optical control of phase shift properties is of special interest, caused by a rapidly increasing market coverage of MMICs and their possible use in future phased array antennas. In particular, the microwave characteristics of optically illuminated GaAs MeSFETs have been shown to be changed by a photovoltaic voltage generated in the gate Schottky-barrier region.[3] On the other hand, the variation of the propagation constant by an optically induced plasma in high-purity semiconductor materials acting as dielectric waveguides seems to be a more direct way.[4] However, the coplanar line is thought to be the most promising waveguide for MMIC applications, and changes in the phase constant[5] or the attenuation constant[6] of coplanar lines on semi-insulating substrate have been obtained by optically varying the local conductivity.

On the other hand, active travelling-wave devices on a semiconducting substrate, such as the Schottky coplanar line, are preferably operated in the slow-mode region, and the capacitance of the distributed depletion layer is varied electrically to achieve phase shift control. These lines have become more and more interesting for phased array applications because it has been shown that the attenuation can be reduced without losing the phase shift capability.[7] Owing to their structure resembling that of a distributed 'travelling-wave' MeSFET, optical control, which would be very interesting from the viewpoint of optoelectronic integrated circuits (OEICs), should easily be possible. In this letter we present first experimental results on the optically controlled properties of Schottky coplanar lines.

Coplanar structure, bias circuit and illumination: The essential details of the experimental set-up are sketched in Fig. 1. The

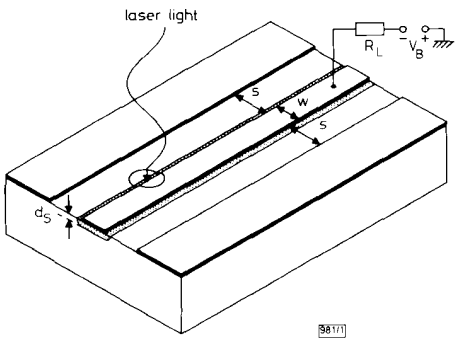

Fig. 1 *Sketch of illuminated Schottky coplanar line*
$s = 30\,\mu m$, $w = 130\,\mu m$

coplanar Schottky-contact transmission line with aluminium metallisation has been formed, using standard photolithographic and etching techniques, on the surface of an *n*-GaAs substrate with doping concentration $N_D = 4 \times 10^{15}\,cm^{-3}$. The centre conductor is reverse-biased using a load resistance $R_L = 500\,k\Omega$ and a reverse bias voltage $V_B = 20$ V. It is well known that in the semiconductor a depletion layer is formed under the centre conductor, the width d_S of which strongly depends on the applied voltage. CW optical illumination of the line is performed using a Ti:sapphire-laser pumped by an ar-ion laser. The wavelength is tuned to 842 nm. Thus the photon energy is slightly greater than the bandgap of GaAs, and electron-hole pairs can be generated. The spot diameter on the probe surface and the incident optical power are about $42\,\mu m$ and 10 mW, respectively. Moving the coplanar line in relation to the laser spot by means of a stepper motor, it is possible to vary the position of optical excitation and to scan longitudinally and transversally to the direction of wave propagation.

Experimental results: The propagation constant of the Schottky coplanar line with and without illumination was determined by conventional network analysis in the frequency range from 0·5 to 8·0 GHz. Without illumination the phase and attenuation constant (which are not shown here) are those of the well known Schottky coplanar line used as an electrically tunable phase-shifter (see, for example, Reference 7 and References therein). By directing the laser spot onto the edge of the reverse-biased centre conductor and thus illuminating the depletion layer, the phase constant was increased over the whole frequency range. In Fig. 2 the difference $\Delta\beta$ of the phase constants with and without optical excitation is presented as a function of frequency *f*. Although the curve, which represents

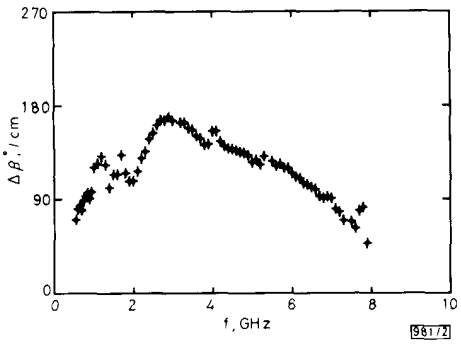

Fig. 2 *Measured values of difference $\Delta\beta$ of phase shifts per unit length of Schottky coplanar line with and without illumination as function of frequency f*

the difference of two measurements, reveals some experimental errors, an optically induced phase shift of the order of 90 to 180°/cm is clearly obtained.

Further experimental details and discussion: Some further experimental details will now briefly be summarised to elucidate the underlying physical mechanism. First, it should be noted that the attenuation constant behaves similar to the phase constant, i.e. over the whole frequency range the losses are enlarged when the edge of the centre conductor is illuminated. Experimentally, it is clearly found that optical control of transmission line properties can only be achieved by illumination of the depletion layer. In contrast, by stepping the laser spot transversally to a Schottky coplanar line with a slot width greater than the spot diameter, no change in phase shift is observed when illuminating only the metallisation, or the edge of the left or right ground conductor, nor when illuminating only the bulk region of the slot. By scanning longitudinally to the line, the degree of variation of the line properties is found to be constant from the input to the output port of the Schottky coplanar line. It is worth mentioning that the degree of variation changes rapidly when the photon energy is tuned in the vicinity of the bandgap. If the wavelength is greater than 884 nm only a slight phase shift can be observed. When the wavelength is decreased from 884 to 871 nm the phase shift increases to a maximum value. This value remains constant when the wavelength is continuously decreased to 840 nm. Likewise a great effect is achieved when varying the optical input power level from no light to the order of 10 mW, whereas a further enhancement of illumination intensity is inefficient.

The biasing conditions, which are essential for the underlying physical mechanism, can easily be detected by measuring the voltage drop across the load resistor and the current. It is found that the dark probe resistance is approximately 470 kΩ, resulting in a voltage drop of 9·7 V across the depletion layer. By illuminating the depletion layer, the probe resistance is reduced to only 35 kΩ, resulting in a reduced voltage of 1·3 V. By that means the depletion layer width is reduced, resulting in a variation of the transmission line properties equivalently to the pure electrical control. In the present case an optimum load resistance R_L can be determined to achieve a maximum phase shift. It is found that R_L depends on different parameters, such as the microwave frequency, but is always of the order of a few hundred kΩ. Thus a novel mechanism is intro-

duced in optically controlled phase-shifters, the device not being a plasma-controlled dielectric waveguide, but rather a structure acting simultaneously as a distributed Schottky photodiode and as a transmission line.

Conclusion: In this letter it has been demonstrated experimentally that the phase shift of Schottky coplanar lines can be optically controlled by illuminating the depletion layer with photon energies greater than the bandgap. It should be further noted that this 'travelling-wave' Schottky photodiode can theoretically be described by the usual quasi-TEM equivalent circuit (see References in Reference 7) including the well known photocurrent source. The presented optoelectronic device may be very interesting in the area of future phased array antennas, especially when electrical isolation and decoupling are required. The fairly high time constant of our nonoptimised line, which is due to the load resistance and the large capacitance of the device, limits the upper modulation frequency to a few tens of kHz, but this is no restriction as compared to mechanical systems. Owing to its structural and technological compatibility with GaAs MeSFETs and metal/semiconductor Schottky-barrier photodiodes, this device may also be very well suited for monolithic microwave optoelectronic circuits (MMOCs).

Acknowledgments: We thank the Deutsche Forschungsgemeinschaft (DFG) and the Bundesministerium für Forschung & Technologie (BMFT) for financial support.

D. KAISER
M. BLOCK
D. JÄGER

Institut für Angewandte Physik
Universität Münster
Corrensstrasse 2/4, D-4400 Münster, Federal Republic of Germany

29th September 1989

References

1 ARJAVALINGHAM, G., PASTOL, Y., HALBOUT, J.-M., and KOPCSAY, G. V.: 'Use of optoelectronically generated transient radiation for broadband dielectric measurements'. PIERS '89, Boston, Conf. proc., Session VIII, pp. 115–116
2 HEIDEMANN, R., and JÄGER, D.: 'Optical injection locking of BARITT oscillators', *IEEE Trans.*, 1983, **MTT-31,** pp. 78–79
3 DESALLES, A. A. A.: 'Optical control of GaAs MESFETs', *ibid.*, 1983, **MTT-31,** pp. 812–820
4 VAUCHER, A. M., STRIFFLER, C. D., and LEE, C. H.: 'Theory of optically controlled millimeter-wave phase shifters', *ibid.*, 1983, **MTT-31,** pp. 209–216
5 ITOH, T.: 'Applications of coplanar transmission line structures for microwave-optical interaction circuits'. MIOP '89 Sindelfingen, Conf. proc. (Network GmbH Hagenburg, 1989), Session 5B
6 PLATTE, W., and SAUERER, B.: 'Optically CW-induced losses in semiconductor coplanar waveguides', *IEEE Trans.*, 1989, **MTT-37,** pp. 139–149
7 KAISER, D., BLOCK, M., LACKMANN, U., and JÄGER, D.: 'Variable phase shift of spatially periodic proton-bombarded Schottky coplanar lines', *Electron' Lett.*, 1989, **25,** pp. 1135–1136

POLYPHASE BARKER SEQUENCES

Indexing term: Information theory

Polyphase sequences are time-discrete complex sequences with constant magnitude and variable phase. In this letter polyphase sequences with aperiodic autocorrelation function (ACF) sidelobes of values less than or equal to 1 are presented. Such sequences are called Barker sequences. Binary Barker sequences with elements 1 or -1 are only known up to 13 elements. Now, with an iteration scheme, polyphase Barker sequences are found up to 25 elements, except for 20 elements.

Introduction: Polyphase sequences are time-discrete complex sequences with constant magnitude and variable phase. In communication, system identification, measurement or radar such finite-length complex sequences with low autocorrelation function (ACF) sidelobes are of interest. The ACF $p(m)$ of a sequence $s(n)$ with N complex elements of magnitude 1 is given by

$$p(m) = \sum_{n=0}^{N-m} h^*(n) \cdot h(n+m) \qquad \text{with } m = 0, \pm 1, \pm 2, \ldots, \pm(N-1) \quad (1)$$

if $h^*(n)$ denotes the complex conjugate of $h(n)$.

If the ACF sidelobes satisfy

$$|p(m)| \leq 1 \qquad \pm 1 \leq m < \pm N \quad (2)$$

the sequence $h(n)$ is called a Barker sequence.

Binary Barker sequences with elements 1 or -1 were first considered in 1953.[1] Binary Barker sequences are only known for lengths $N = 2, 3, 4, 5, 7, 11$ and 13. Further binary Barker sequences can only exist for length $N = 4C^2$, with C an integer. It is well known that such Barker sequences do not exist for $C \leq 55$ or $N \leq 12\,100$.[2]

Binary sequences can be regarded as complex sequences with elements of magnitude 1 and two-valued phases. If the elements of finite complex sequences with magnitude 1 are taken from a larger alphabet, the sequences have more degrees of freedom, e.g. quaternary sequences with elements $+1$, i, -1, $-i$ or sextic sequences. Golomb *et al.* dealt with transformations from binary to ternary, quaternary and sextic Barker sequences.[3] However, in Reference 3 ternary Barker sequences could only be found up to length 9, quaternary Barker sequences up to length 15 and sextic Barker sequences up to length 13.

N-phase sequences have elements, which are taken from an alphabet $(2\pi/N)i$, $0 \leq i \leq N$, which increases proportional to the number of elements. Construction methods for generating N-phase sequences with low ACF sidelobes are not known. So far, N-phase sequences with low ACF out-of-phase values have been obtained by testing every cyclic shift of a sequence with good periodic ACF properties.[4–6]

In Reference 7 applications of numericals methods for minimising functions of continuous-valued variables were used to find the phases of a polyphase sequence with low ACF sidelobes. Polyphase Barker sequences could be found up to 18 elements. For larger N such algorithms become computationally expensive, because they have the disadvantage that they first construct the sequence and then test their ACF properties.

Therefore, in this letter another way is given. An iterative algorithm, which is based on constrained iteration techniques, is applied to generate polyphase Barker sequences.[8,9]

Iteration scheme: The $2N$-point discrete Fourier transform (DFT) $H_i(k)$ of the complex sequence $h_i(n)$ of length N is calculated after setting the elements $h_i(n)$ to zero for $N \leq n < 2N$.

Suppose $P(k)$ is calculated by the $2N$-point DFT of the ACF $p(m)$, where m is reduced mod $2N$ and $P(N)$ is set to zero. The frequency-domain sequence $P(k)$ can then be expressed by

$$P(k) = H^*(k) \cdot H(k) = |H(k)|^2 \qquad 0 \leq k < 2N \quad (3)$$

To compute polyphase sequences with low ACF sidelobes, an iterative method is built up which incorporates the basic relation of eqn. 3 in four steps:

(1) Calculate the ACF $p_i(m)$ of the ith estimate $h_i(n)$.

(2) Obtain with mapping A the new ACF $\hat{p}_i(m)$ with lower sidelobes, and calculate its $2N$-point DFT $\hat{P}_i(k)$.

(3) Apply mapping B to the $2N$-point DFT $H_i(k)$ of the ith estimate $h_i(n)$ to obtain the sequence $G_i(k)$ by incorporating $|P_i(k)|$.

(4) Apply mapping C to the sequence $g_i(n)$, which is built by the inverse DFT of $G_i(k)$. Then the next estimate $h_{i+1}(n)$ of $h(n)$ is generated. By setting $i + 1$ to i the iteration loop is closed.

With mapping A selected ACF sidelobes are manipulated. To obtain polyphase sequences with low ACF sidelobes, two